Quantitative Electron Spectroscopy of Surfaces:

A Standard Data Base for Electron Inelastic Mean Free Paths in Solids

M. P. Seah and W. A. Dench
Division of Chemical Standards, National Physical Laboratory, Teddington, Middlesex, UK

A compilation is presented of all published measurements of electron inelastic mean free path lengths in solids for energies in the range 0–10 000 eV above the Fermi level. For analysis, the materials are grouped under one of the headings: element, inorganic compound, organic compound and adsorbed gas, with the path lengths each time expressed in nanometres, monolayers and milligrams per square metre. The path lengths are very high at low energies, fall to 0.1–0.8 nm for energies in the range 30–100 eV and then rise again as the energy increases further. For elements and inorganic compounds the scatter about a 'universal curve' is least when the path lengths are expressed in monolayers, λ_m. Analysis of the inter-element and inter-compound effects shows that λ_m is related to atom size and the most accurate relations are $\lambda_m = 538E^{-2} + 0.41(aE)^{1/2}$ for elements and $\lambda_m = 2170E^{-2} + 0.72(aE)^{1/2}$ for inorganic compounds, where a is the monolayer thickness (nm) and E is the electron energy above the Fermi level in eV. For organic compounds $\lambda_d = 49E^{-2} + 0.11E^{1/2}$ mg m^{-2}. Published general theoretical predictions for λ, valid above 150 eV, do not show as good correlations with the experimental data as the above relations.

INTRODUCTION

The chemical analysis of the surface and near-surface regions of solids by electron spectroscopy, for example Auger electron spectroscopy, X-ray and UV photoelectron spectroscopies, is now a routine operation. The measurements are generally made quantitative, in terms of the composition averaged over the spectroscopy's sampling depth, by relating the intensities measured to those for bulk reference standards.[1–9] However, if it is required to measure the composition of the outermost atom layer, as in adsorption and segregation studies, before applying this procedure it is necessary to know the electrons' sampling depths, so that the contribution to the signal from atoms in each atom layer may be determined. This depth of analysis can be directly derived from the electrons' inelastic mean free paths (IMFPs) and a knowledge of the analysis geometry.[10,11] The accuracy of the final quantitative result for the composition of the surface atom layer depends directly on the accuracy with which the IMFP is known.

There are two methods currently used for obtaining the IMFP: experimental determination and theoretical prediction. There are currently about 350 measurements of IMFPs in different materials at different energies, one general set of theoretical predictions and several calculations for particular materials. At some point, therefore, the prospective analyst of the surface atom layer must either perform his own direct calibration experiment, which is as difficult as an IMFP determination, or he must choose between one of the above ways of obtaining his IMFP from the literature. This work sets out to simplify his choice and provide a recommended means for determining both the value for the IMFP which is likely to incur the least error and the value of that error. Use of this recommendation will enable the accuracy of adsorbate level measurements to be improved and the comparison of results between different workers will be made more meaningful, since they will no longer be using different values of IMFP for the same material.

In the section that follows, a compilation of all the published data of IMFPs is described. The degree of correlation between the measured IMFPs and simple empirical functions of electron energy and material parameters is then examined to determine which function best fits the data. The goodness of fit is then compared with that of the available theoretical predictions to define the method which gives the best description of the experimental data.

THE COMPILATION

Compilations of IMFPs have been presented in the past by several authors, but the most useful are those of Lindau and Spicer,[12] with data in the energy range 0–3000 eV above the Fermi level, and of Powell,[13] with data between 40 and 3000 eV. The analysis of experimental results by these authors shows that the IMFP has a minimum value for energies around 100 eV and that at higher energies it varies 'roughly as the square root of electron energy'. Powell's compilation consisted of 57 data points which describe a 'universal' trend with a broad scatter. In that work it was not clear if the scatter was mainly due to experimental error or to differences in the materials studied. It was not clear whether a 'universal curve' should exist and, if so, whether the real scatter about this curve for different materials would be greater or smaller than the accuracy of current theoretical predictions for these materials.

Since Powell's compilation many more values of IMFPs have become available and the total is now nearly 350. These values allow a more accurate assessment of

CCC-0142-2421/79/0001-0002$05.00

IMFPs and their dependence on material and energy. Also, by increasing the energy range considered to include data down to zero eV, the low energy deviation from the square root of energy dependence may be more accurately defined. All currently available values of IMFPs have been accumulated into a computer store so that at any time the fullest compilation of data is readily available. All data have been included without reference to the author's estimates of error and no data have been rejected on the grounds of poor experimental technique or excessive divergence from the mean. A list of the references, with a note of the material studied, is given in the Appendix. Comments on the experimental techniques and their relative merits will not be given here as they are suitably covered by Powell.[13] It is assumed that all the random errors will be removed by averaging over the large number of results whilst systematic errors are commented on later in this section.

The data stored for each measurement include the material through which the electron passes, this material being grouped under one of the four titles: elements, inorganic compounds, organic compounds and adsorbed gases. The rest of the data consists of the electron energy above the Fermi level in eV (E), the IMFP in nanometres (λ_n), the IMFP in monolayers (λ_m), the IMFP in milligrams per square metre (λ_d) and another parameter, λ_a, to be described later. Where electron energies are given by XPS and UPS users the Fermi level is the customary reference level; however, AES users refer to the apparent vacuum level, not adjusted for the contact potential difference between their sample and the analyser system. The average addition necessary to reference AES work to the Fermi level is about 4 eV,[14] so this has been added, where necessary, to AES energy values. The IMFP values in nanometres have generally been calculated from the original curves or published values, making due allowance for the geometrical factors relating to the sample and analyser disposition.[10,11] Conversion of the IMFP from λ_n to λ_m is accomplished via the relation

$$\lambda_n = a\lambda_m \tag{1}$$

where the monolayer thickness, a (nm), is given by

$$a^3 = \frac{A}{\rho n N} \times 10^{24} \tag{2}$$

where A is the atomic or molecular weight, n is the number of atoms in the molecule, N is Avogadro's number and ρ is the bulk density in kg m^{-3}.[14,15] Conversion to λ_d is accomplished via the relation

$$\lambda_d = 10^{-3}\rho\lambda_n \tag{3}$$

This approach ignores structure. In LEED studies, where the surface structure is defined, the IMFP is usually presented directly in terms of monolayers. In the LEED study the number of atoms per square metre (N_s) in the monolayer is usually known and λ_d is then given by

$$\lambda_d = \frac{10^3 A N_s}{N n}\lambda_m \tag{4}$$

Subsequently λ_n is derived via Eqn (3).

The measurements for elements are shown in Fig. 1(a–c). Clearly, for establishing a universal curve, the expressions in terms of nanometres and monolayers are much better than that in mg m^{-2}. Least squares analysis shows that the measurements for energies below 15 eV are described by a power law not significantly different from E^{-2} and those above 75 eV by $E^{1/2}$. For inorganic compounds the results are similar and, for brevity, only the measurements in nanometres are shown in Fig. 1(d). Again, above 75 eV, the $E^{1/2}$ law holds. At low energies and for organic compounds and adsorbed gases, shown in Fig. 1(e and f), the results are too few to establish meaningful power laws and so they are assumed to be the same as those exhibited by the elements.

Superimposed on the compilations shown in Figs. 1(a)–(f) are the least squares fits to the general relation

$$\lambda_i = \frac{A_i}{E^2} + B_i E^{1/2} \tag{5}$$

where i = n, m or d. A_i and B_i for the different materials groups and expressions of λ_i are given in Table 1. Also shown in Table 1 is the number of relevant data points and their RMS scatter factor about the empirical least squares fit. Because the measurements appear with even scatter on the log-scaled plots of Fig. 1, all the least squares fits and RMS deviations were calculated in terms of ln λ. The RMS deviation for ln λ becomes a multiplying factor for λ, here called the RMS scatter factor.

It may be seen in Fig. 1(a and b) that there is a transition region from 10 to 100 eV where the results are scarce and scattered. Systematic errors are probably greatest here. Nearly all XPS work and much AES work requires data not in this region but above 100 eV. The transition region appears to be well cleared by 150 eV and so least squares fits were obtained for

$$\lambda_i = B_i E^{1/2} \qquad E > 150 \text{ eV} \tag{6}$$

for the materials groups for energies above 150 eV. These B values appear in Table 1. The B values obtained in fitting Eqn (5) over all energies differed from these B values by less than 3% and so, to reduce the number of empirically determined variables, the B values from Eqn (6) were used in establishing the least squares fits for A in Eqn (5).

It is clear from Table 1 that, for elements, the best estimate of IMFP is given by λ_m with the experimental values having an RMS scatter factor of 1.38 about this curve for energies above 150 eV. The results for gold, which has 22 data points from 6 different experiments, indicate that a factor of 1.30 may be due to experimental inaccuracies. The remaining factor of 1.20 must be attributed to inter-element differences which are considered below. For inorganic compounds λ_m is again the best measure, but here the coefficient B_m is 1.74 times that for elements.

For both AES and XPS, analysis of the important inter-element differences is best restricted to the data above 150 eV. Using Eqn (6) for λ_n, an average B_n value for each element may be calculated. The ratio of this B_n value to the overall average B_n for all elements is a measure of the deviation of the particular element's IMFP from the mean. This ratio, R_n, may be assessed empirically against many parameters. R_n is greater than unity for the alkali metals, around unity for Cu, Ag, Au, Zn and Al, and less than unity for the transition metals. Possible simple parameters which could give this type of dependence are: conduction band electron density n_e,

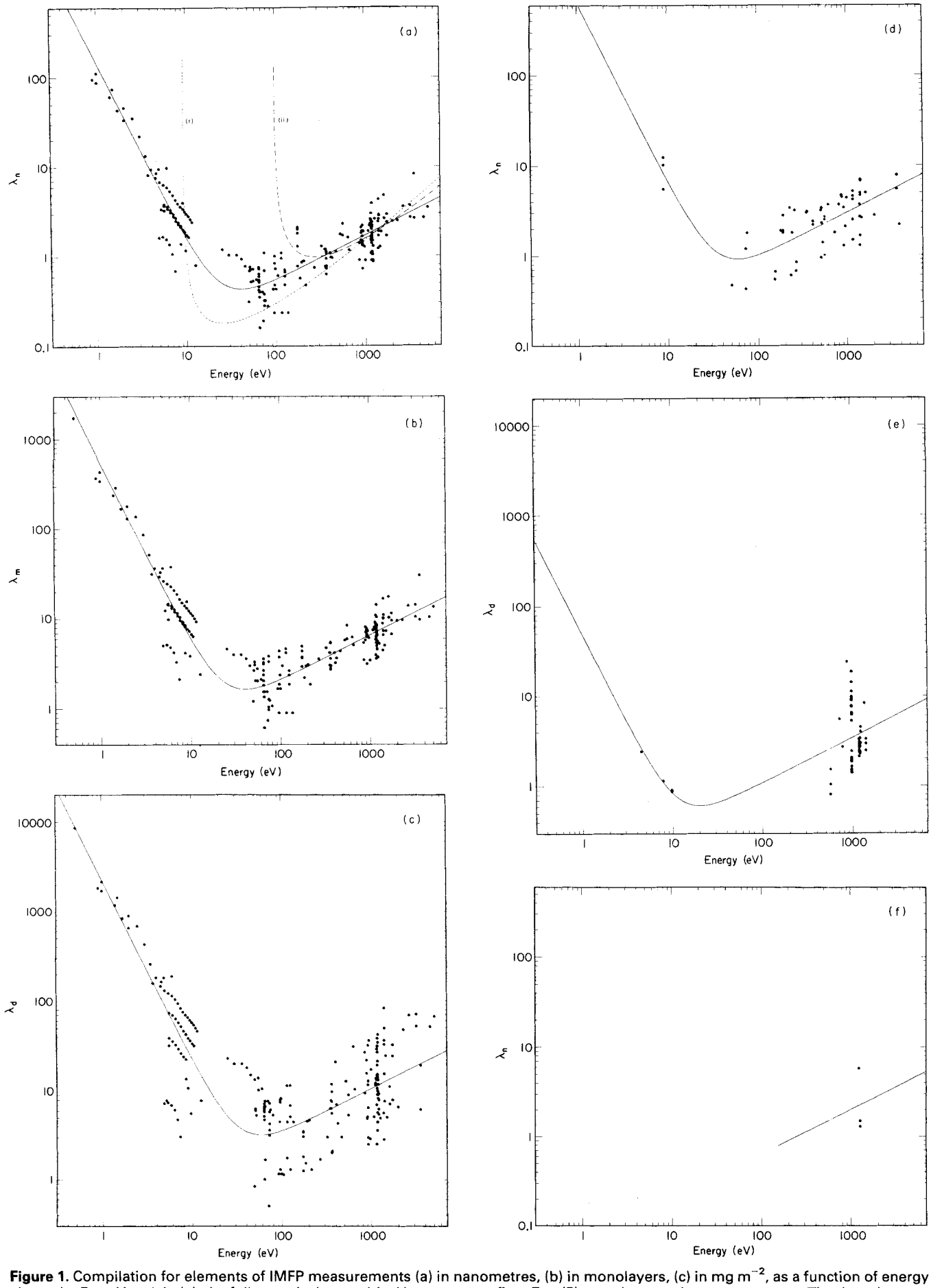

Figure 1. Compilation for elements of IMFP measurements (a) in nanometres, (b) in monolayers, (c) in mg m^{-2}, as a function of energy above the Fermi level. In (a), the full curve is the empirical least squares fit to Eqn (5) over the complete energy range. The dotted curves are for Penn's relation (24) with (i) his mean values for *a* and *b*, (ii) values of *a* and *b* to give the least squares fit to the data above 150 eV. (d) Compilation for inorganic compounds of IMFP measurements in nanometres. (e) Compilation for organic compounds of IMFP measurements in mg m^{-2}. (f) Compilation for adsorbed gases of IMFP measurements in nanometres.

Table 1. *A* and *B* values for Eqns (5) and (6) for the IMFPs

Equation (6) *for energies above* 150 *eV*

Material	No. of results	λ_n B_n	RMS	λ_m B_m	RMS	λ_d B_d	RMS	λ_a B_a	RMS
Gold	22	0.054	1.30	0.209	1.30	1.036	1.30	0.41	1.30
Elements	102	0.054	1.47	0.210	1.38	0.336	2.23	0.41	1.36
Inorganic compounds	52	0.096	1.70	0.365	1.47	0.298	1.56	0.72	1.38
Organic compounds	57	0.087	2.12			0.110	2.10		
Adsorbed gases	3	0.064	1.98						

Equation (5) *for all energies* (for *B* values see above)

Material	No. of results	λ_n A_n	RMS	λ_m A_m	RMS	λ_d A_d	RMS	λ_a A_a	RMS
Gold	82	177	1.48	688	1.48	3400	1.48	1360	1.48
Elements	215	143	1.57	538	1.59	2220	2.44	1040	1.61
Inorganic compounds	59	641	1.70	2170	1.48	3630	1.53	3990	1.40
Organic compounds	61	31	2.07			49	2.05		

atom size a, number of conduction band electrons per atom N_v, or some combination of these. Regression analysis, weighting the ratio R_n for each element by the number of measurements for that element, gives

$$R_n \propto n_e^{-0.26} \quad (7)$$

$$R_n \propto a^{1.6} \quad (8)$$

$$R_n \propto N_v^{-0.46} \quad (9)$$

Now it is well known that as N_v rises, a generally falls, so the above dependences are not independent and must be studied sequentially. The least scatter occurs for relation (8) which is not significantly different from an $a^{3/2}$ dependence, as shown in Fig. 2. Note that the points for Au, Al, Ag, Ge and Si have much heavier weighting than the others. The $a^{3/2}$ dependence can be removed by considering $R_n a^{-3/2}$ to test for the residual dependence on N_v. In Fig. 3, $R_n a^{-3/2}$ is shown plotted against N_v and there is clearly no significant relation between the two. From relation (8) one can see why the scatter factor for Eqn (6) decreases through the series λ_d to λ_n to λ_m and that $\lambda_m a^{-1/2}$ should have the least scatter of all. Analysis gives

$$\lambda_m = 0.41(aE)^{1/2} \quad [1.36] \quad (10)$$

where the figure in square brackets is the RMS scatter factor. The term $\lambda_m a^{-1/2}$ is written as λ_a, the parameter mentioned earlier. From Eqn (6) B_a values can be obtained and thence R_a values. The distribution of R_a values for each measurement on each element is shown in Fig. 4. It is clear from Fig. 4 that, as the results from groups such as the alkali metals, or the sets of results for Si, Al or Au each independently span the whole distribution, the majority of the remaining scatter in the histogram is probably a result of experimental inaccuracies.

A similar analysis to that above, for inorganic compounds, is shown in Fig. 5, again with R_n propor-

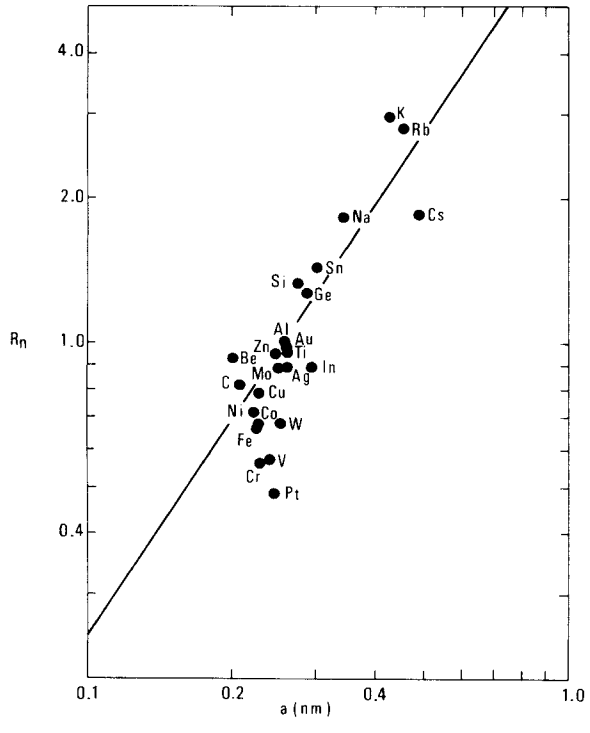

Figure 2. The deviation of R_n from the mean for various elements as a function of atom size, for energies above 150 eV.

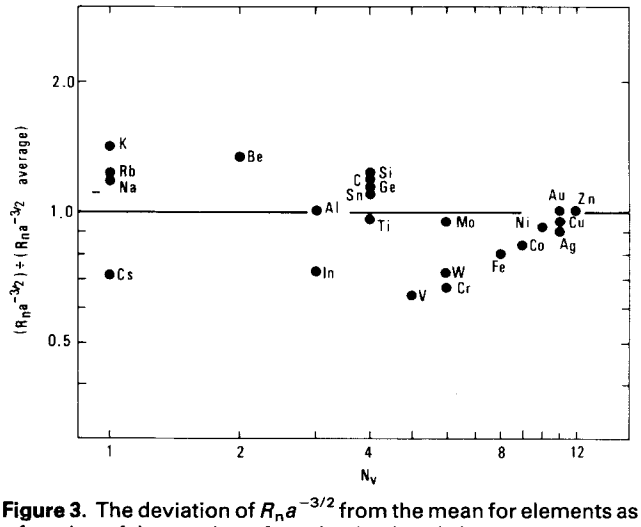

Figure 3. The deviation of $R_n a^{-3/2}$ from the mean for elements as a function of the number of conduction band electrons per atom, for energies above 150 eV.

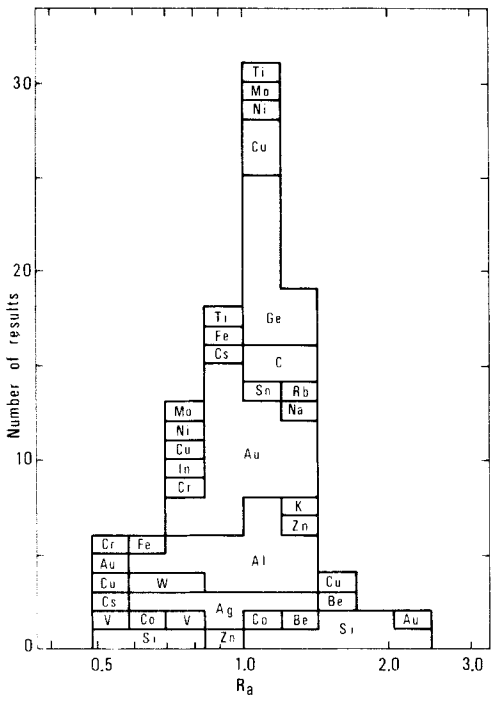

Figure 4. The distribution of R_a for each measurement on an element about the mean, for energies above 150 eV.

tional to $a^{3/2}$ for measurements at energies above 150 eV. Thus, for inorganic compounds

$$\lambda_m = 0.72(aE)^{1/2} \qquad [1.38] \qquad (11)$$

again with no dependence on N_v. The values of A_a and B_a for Eqn (5) are shown in Table 1 for elements and inorganic compounds. The averages for the B_a distributions for the elements and inorganic compounds are separated by 1.76 standard deviations and Student's t-analysis shows that the probability that the elements and inorganic compounds are indeed separate classes exceeds 99.9%. The universal curves for λ_a for the elements and inorganic compounds are shown in Figs. 6(a) and (b) respectively. Although values of A_a are given in Table 1, analysis of the dependence of λ_m for energies below 20 eV shows that there is no significant correlation with a. Thus the recommended relation for elements for all energies contains the $a^{1/2}$ dependence only in the high energy term. Hence

$$\lambda_m = \frac{538}{E^2} + 0.41(aE)^{1/2} \qquad [1.36] \qquad (12)$$

and for inorganic compounds

$$\lambda_m = \frac{2170}{E^2} + 0.72(aE)^{1/2} \qquad [1.38] \qquad (13)$$

where the scatter factors apply to $E \geq 150$ eV.

The analysis for organic compounds cannot be made in terms of λ_m or λ_a as a meaningful a value cannot be

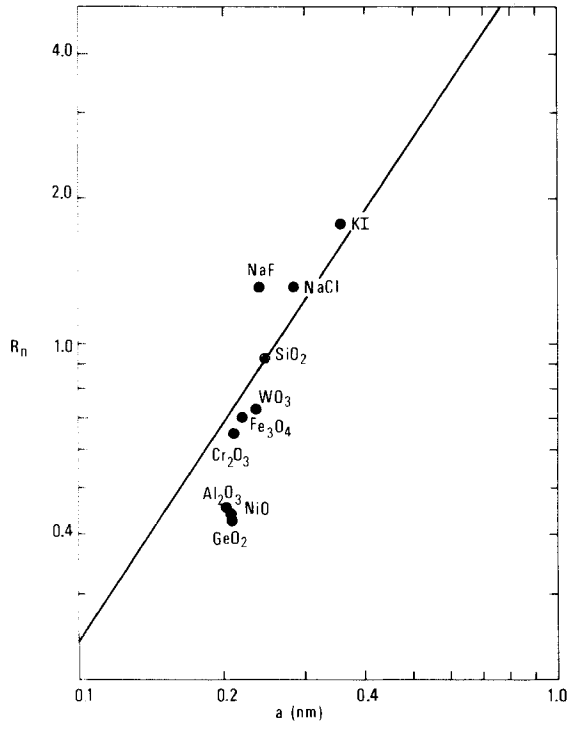

Figure 5. The deviation of R_n from the mean for inorganic compounds as a function of atom size, for energies above 150 eV.

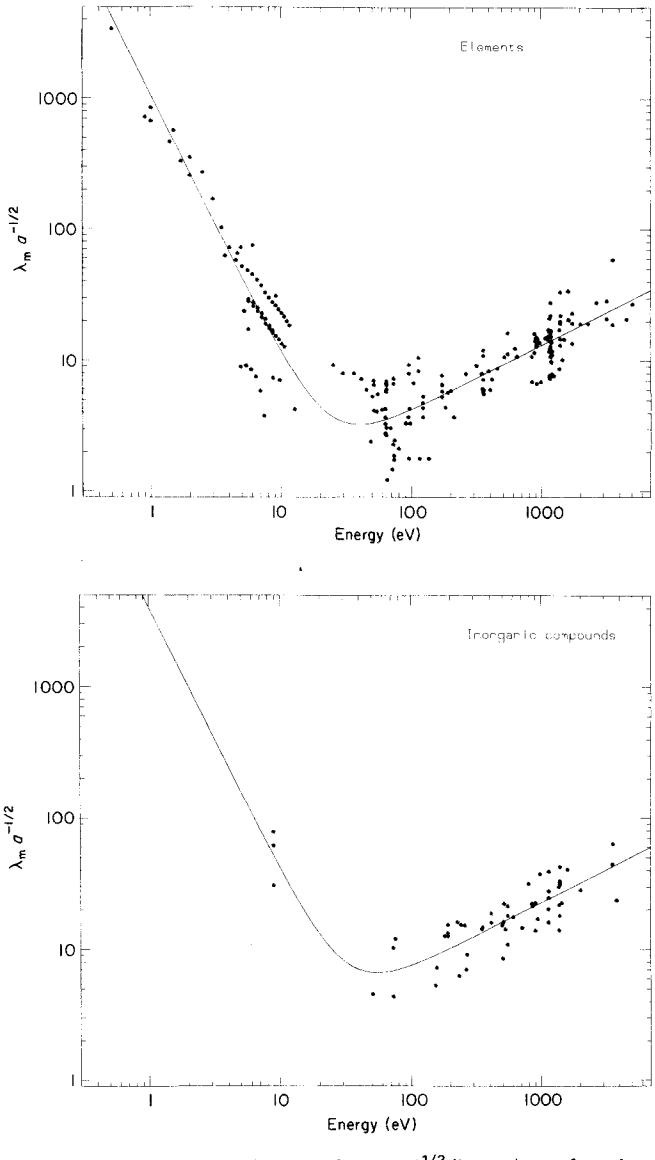

Figure 6. Compilation of results for $\lambda_m a^{-1/2}$ (i.e. λ_a) as a function of electron energy for (a) elements, (b) inorganic compounds.

defined. The least scatter occurs for λ_d:

$$\lambda_d = \frac{49}{E^2} + 0.11E^{1/2} \qquad [2.10] \qquad (14)$$

For gases, values of A_n and B_n occur in Table 1. However, these values are based on an analysis of only three results and are likely to be less accurate than the estimate for the nearest equivalent from the appropriate element or compound.

THEORY

There are two aspects of theory involved here; one describes how the IMFP is used in quantitative analysis of adsorbates, the other concerns the derivation of the IMFP as a function of energy and material from a knowledge of the electron states in the solid.

(a) The IMFP and quantitative analysis of adsorbates

In this section quantification is considered with reference to spectra from bulk standards. For an incoherent scattering model of a uniformly adsorbed layer of A, of monolayer thickness, covering a fraction X of the surface of a substrate B, the intensities of the characteristic electrons, along a direction at an angle θ to the surface normal, are given by

$$I^A = XI^A_\infty \left\{\frac{1+r_B(E_A)}{1+r_A(E_A)}\right\}\left\{1-\exp\left(\frac{-\sec\theta}{\lambda^A_m(E_A)}\right)\right\} \qquad (15)$$

and

$$I^B = I^B_\infty \left\{1 - X + X\exp\left(\frac{-\sec\theta}{\lambda^A_m(E_B)}\right)\right\} \qquad (16)$$

where I^A_∞ and I^B_∞ are the signals from pure bulk standards for the adsorbate and substrate respectively, $r_A(E_B)$ and $\lambda^A_m(E_B)$ are respectively the backscattering contribution and the IMFP (monolayers) of B Auger electrons in the matrix of A. For XPS the r's are zero but for AES they are in the range 0.1–0.6.[16]

For $\lambda \gg a$, a continuum model may be used instead of the above layer-by-layer model. For a thickness of m monolayers of adsorbate

$$I^A = I^A_\infty \left\{\frac{1+r_B(E_A)}{1+r_A(E_A)}\right\}\left\{1-\exp\left(\frac{-m\sec\theta}{\lambda^A_m(E_A)}\right)\right\} \qquad (17)$$

$$I^B = I^B_\infty \exp\left(\frac{-m\sec\theta}{\lambda^A_m(E_B)}\right) \qquad (18)$$

For $\lambda \gg a$ and for $r_A = r_B$, the above pairs of equations reduce to

$$\frac{I^A}{I^A_\infty} = \frac{m}{\lambda^A_m(E_A)\cos\theta} \qquad (19)$$

$$\frac{I^B}{I^B_\infty} = 1 - \frac{m}{\lambda^A_m(E_B)\cos\theta} \qquad (20)$$

where, if m is less than unity, it becomes the fraction X of Eqns (15) and (16). For adsorption work the direct relevance of λ_m, rather than λ_n or λ_d, is clear.

Because, in quantification using separate bulk standards, all operating conditions and surface textures must be held constant, an alternative technique, using the relative intensities from a dilute binary alloy of A in B, is often used. To obtain the same composition at the surface as in the bulk, the sample is generally a single crystal cleaved in the UHV of the spectrometer just before analysis. This technique has the additional advantage for AES that the backscattered electron energy spectrum impinging on A atoms is the same in the solute and adsorbate states. Thus the factor involving the r's approaches unity. If the solute molar fractional content is X_A, the same adsorbate-to-substrate relative signal would be obtained for a fractional surface coverage X given, for $\lambda \gg a, b$, by

$$X = \frac{a^2}{b^2}\left(\frac{X_A}{1-X_A}\right)\lambda^B_m(E_A)\cos\theta \qquad (21)$$

where a and b are the respective atom sizes.

Thus, in both of these approaches using bulk standards for quantifying adsorbed layers, the IMFP (monolayers) is of first-order importance. In many of the experiments to measure the IMFP the above arguments are reversed, ancillary experiments are used to quantify the adsorbate level and the equations may then be used to derive $\lambda\cos\theta$. In many papers the term 'attenuation length' is used and it is often not clear if λ or $\lambda\cos\theta$ is intended. *It is recommended that the term 'escape depth' be used for the function $\lambda\cos\theta$ and 'inelastic mean free path' for the more fundamental λ.*

In XPS work the electron spectrometers used for IMFP determination have small apertures and well-defined $\cos\theta$ values. For AES work the cylindrical mirror analyser (CMA) and retarding field analyser (RFA) are customarily used so that the intensities should be integrated over the collection angle. For the CMA, with its axis along the surface normal and up to about 45° from the normal, Seah[10] and Shelton[11] find an effective $\cos\theta = 0.74$. For the RFA of semi-vertical angle 60° along the surface normal, $\cos\theta = 0.74$ again.[10] For other conditions lower values generally occur. The integrals over angle assume an isotropic distribution of electrons from the source atom and are evaluated numerically. The results are a sum of many exponentials and do not always give a final simple exponential relation, such as Eqn (18), as the adsorbate builds up. The above values for the effective $\cos\theta$ are for the substrate intensity to fall to $1/e$. The exact curves for many specific instances are given by Seah,[10] Shelton[11] and Norman and Woodruff.[17]

For very low energy electrons refraction at the surface potential causes a limit to the range of θ's in the adsorbate layer that may be detected by an external analyser. In the nearly free electron approximation this would increase the effective $\cos\theta$ appropriate to most experiments. However, experiments by Seah[18] and Krolikowski and Spicer[19] show that the probability of transmission of low energy electrons through the surface barrier is much higher than expected by the above model and so the surface refraction has been ignored in calculating IMFPs for the compilation.

(b) The theoretical prediction of IMFPs

The IMFP (λ) commonly used in AES and XPS studies is the characteristic path length involved when the elec-

tron's probable decay in intensity is given by

$$I = I_0 \exp(-x/\lambda) \tag{22}$$

where x is the displacement of the electron from its point of origin. Because of elastic scattering of the electron, Eqn (22) is true only if x is the total distance travelled by the electron. If the elastic scattering is incoherent and isotropic, an average electron path that is broken into n steps by $(n-1)$ elastic scattering events will give an average displacement $n^{-1/2}\lambda_i$, where λ_i is the path length for inelastic scattering. If the path length for elastic scattering is λ_e, the probability of any given number of elastic scattering events, n, can be calculated in terms of the ratio s, equal to λ_i/λ_e. If n, in Eqn (22), is the net displacement from the point of origin,

$$\lambda = \frac{\lambda_i}{(1+s)}\left\{1+\frac{1}{\sqrt{2}}\left(\frac{s}{1+s}\right)+\frac{1}{\sqrt{3}}\left(\frac{s}{1+s}\right)^2+\cdots\right\}$$

For $s \leqslant 1$, this series closely approximates

$$\lambda = \lambda_i/(1+s)^{0.293}$$

From studies of the secondary electron energy spectrum from polycrystalline or amorphous solids it is seen that the reflection coefficient for primary electrons rarely exceeds a few percent, even for very low electron energies.[20] If reflection at the surface barrier is ignored, this coefficient approaches s so that the error in the assumption $\lambda = \lambda_i$ is less than 3% even down to 5 eV above the Fermi level. Therefore, in the rest of this work, elastic scattering will be ignored.

(i) The IMFP at low energies. For very low electron energies, the variation of IMFP with energy is given as a simple approximate analytical function by Quinn[21] and by Sze *et al.*[22] as

$$\lambda \propto E^{-2} \tag{23}$$

Sze *et al.* give a simple alternative derivation as follows: the scattering probability of the excited electron is proportional to the product of accessible filled electron states ($\simeq En(E_F)$) and the accessible unoccupied states ($\simeq En(E_F)$) so that Eqn (23) follows directly.

(ii) The IMFP for energies above 150 eV. A number of calculations of IMFPs appear in the literature. Many of these are summarized by Penn[23] in his analysis of the scattering of energetic electrons by conduction band electrons. For nearly-free-electron materials, i.e. those exhibiting well-defined plasmon losses close to the free-electron value, Penn[24] finds, for energies over 150 eV

$$\lambda_v = \frac{E}{a_v(\ln E + b_v)} \tag{24}$$

where, for many systems with λ in nanometres, a_v is given approximately as $270(\frac{4}{3}\pi a_0^3 n_e)^{1/2}$, a_0 being the Bohr radius (m) and n_e the conduction band electron density (electrons m^{-3}). b_v is also dependent on n_e and rises from -3 for materials with high conduction band electron density to near zero for the alkali metals.

Materials which are not composed of transition or noble metal atoms should fit the above equation. Powell[13] earlier gave a similar relation, but for core level excitation

$$\lambda_c = \frac{E}{\frac{3.92\rho}{A}\sum_j \frac{N_j}{\Delta E_j}\left(\ln E - \ln\frac{\Delta E_j}{4}\right)} \tag{25}$$

where the summation is over the core levels, j, with N_j electrons in the level able to receive an average excitation energy ΔE_j. ΔE_j is assumed by Penn to be twice the core level binding energy for levels of up to 70 eV binding energy and 70 eV more than the binding energy for more tightly bound levels.

In general, $\lambda_c > \lambda_v$ and only the outermost core level is important. The total IMFP is then given by

$$\frac{1}{\lambda_n} = \frac{1}{\lambda_v} + \frac{1}{\lambda_c} \tag{26}$$

and λ_n may be written in the form of Eqn (24). Penn tabulates the a_n's and b_n's for all elements so that λ_n can be determined as a function of electron energy. He extends the calculation to compounds by a direct extension of the effects of the constituent atoms. From Penn's tabulation a typical element has $a_n = 140$ and $b_n = -2.23$. Equation (24) with these values describes curve (i) in Fig. 1(a). In the middle energy range, at about 700 eV, the energy dependence has a power of 0.77 instead of the empirical 0.5.

For many elements $\lambda_c \simeq 5\lambda_v$ and λ_v dominates the IMFP. Since $a_v \propto n_e^{1/2}$, λ_n should be proportional to $(a^3/N_v)^{1/2}$. The relation of λ_n to $a^{3/2}$ is upheld by Figs. 2 and 5 but that to $N_v^{-1/2}$ is not confirmed by Fig. 3. The lack of dependence on N_v may be due to experimental error or it may entail a breakdown of the nearly-free-electron approximation used in the calculations. In the next section Penn's predictions and the simple empirical expressions (12), for elements, and (13), for inorganic compounds, are analysed to see which gives the best agreement with the compiled data.

(c) Comparison of Penn's predictions and experiment

The most direct way of assessing the divergence of the experimental results from Penn's predictions is to consider the ratio, R_P, between each measurement listed in the compilation and Penn's prediction for that element or compound at that energy. The comparison is limited to measurements at energies above 150 eV as the Born approximation used in the theory is not valid for measurements at much lower energies. Analysis of the distributions of R_P and the similar parameter R_a, the ratio to the empirical prediction of Eqn (10), are considered first for gold, the element for which most data exist. Penn's predictions appear to be a factor 1.19 too low and give an RMS scatter factor of 1.37 for the experimental results whereas the equivalent numbers for the empirical prediction through R_a are lower at 1.00 and 1.30 respectively.

Similar analyses to those for gold may be constructed in histogram form for the elements for both R_P and R_a, as shown in Figs. 7 and 4 respectively. Penn's mean prediction is 1.12 too low with an RMS scatter factor of 1.45 whereas the empirical prediction numbers are 1.00 (this figure will automatically be unity) and only 1.36

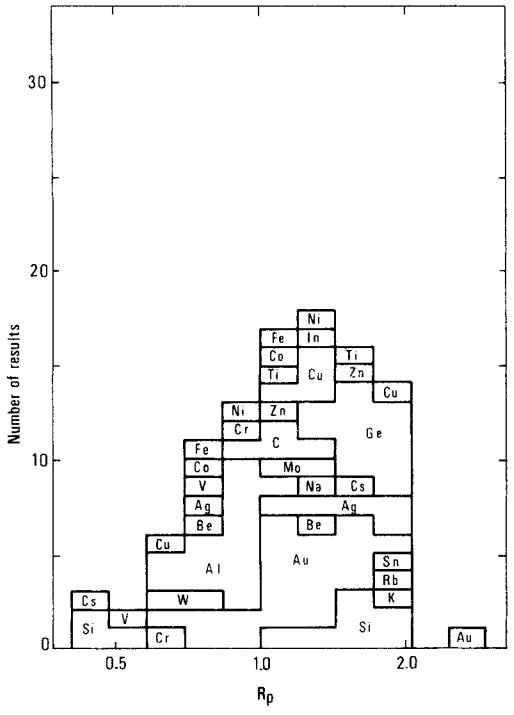

Figure 7. The distribution of the IMFP measurements for all elements about the predictions of Penn,[24] for energies above 150 eV.

respectively. The narrower distribution for the empirical relation (10) arises for two reasons: the differences between elements and also the energy dependence of λ appear to be better described by the empirical equation. The latter point may be noted from the narrower distributions for Au, Ge and C in Fig. 4 compared with only Al being narrower in Fig. 7.

The results for inorganic compounds may be analysed similarly, although the results are much fewer and much of the data comes from only one research group. Histograms for R_P and R_a are shown in Fig. 8(a and b) and, although the results for each compound are tightly grouped, R_P averages 1.92 with an RMS scatter factor of 1.60 whereas R_a averages 1.00 with a scatter factor of only 1.38. Similar calculations to Penn's, but more detailed, were made by Leckey and co-workers for their measurements on Al_2O_3,[25] NaCl,[26] NaF[26] and KI.[26] No attempt was made to generalize the computation so simple extension to other materials is not possible. For the above materials R_L, the ratio of the experimental results to Leckey *et al.*'s predictions, is shown in Fig. 8(c). R_L is on average 1.18 with an RMS scatter factor of 1.36.

Thus, the simple empirical expressions predict the compiled data with better accuracy and lower scatter than do Penn's general predictions and with an accuracy equal to that of Leckey *et al.*'s calculations but with a wider applicability. Equations (12) and (13) therefore predict the measured values for elements and inorganic compounds most accurately. It should be stressed at this point that the above analysis does not prove that the theoretical predictions are in any way inadequate or inaccurate. The experiments to determine IMFPs are very difficult and it is usually not possible to assess the experimental errors since the most important information, the adsorbate morphology, cannot usually be

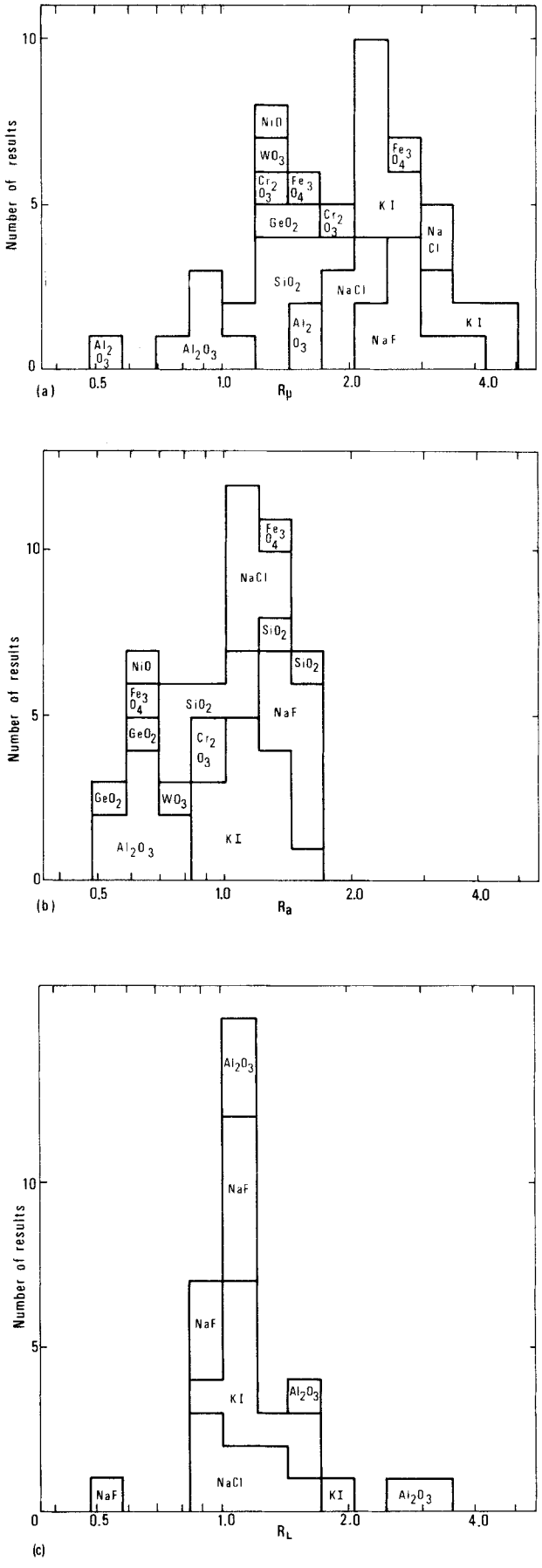

Figure 8. The distribution of the IMFP measurements for inorganic compounds about the predictions of (a) Penn,[24] (b) the empirical equation (11), and (c) Leckey *et al.*[25,26] for energies above 150 eV.

Table 2. a and b values for Eqn (24) (for energies above 150 eV)

Material	No. of results	λ_n a_n	λ_n $-b_n$	RMS	λ_m a_m	λ_m $-b_m$	RMS	λ_d a_d	λ_d $-b_d$	RMS
Gold	22	328	5.04	1.32	84.3	5.04	1.32	17.0	5.04	1.32
Elements	102	271	4.59	1.44	62.4	4.36	1.38	15.5	1.00	2.16
Inorganic compounds	52	126	4.18	1.74	32.5	4.17	1.49	44.2	4.36	1.59
Organic compounds	57	158	4.59	2.13				125	4.59	2.10
Adsorbed gases	3	219	4.59	1.98						

monitored independently. As more data accumulate, the above conclusions will be continually reviewed and any significant changes reported.

To test the general form of Eqn (24), the coefficients a and b were determined by a least squares fit to the measurements on elements for energies above 150 eV. The RMS scatter factor was similar to that for the empirical function (there now being two adjustable parameters) and the result showed, in the 500–1000 eV energy range, an exponent of E of 0.55, much closer to the 0.5 of the empirical relationship than to Penn's 0.77. The curve for this function is shown in Fig. 1(a) and just outside the 150 eV limit it diverges rapidly from the experimental measurements. The values of a and b and the RMS scatter factor for gold and the four materials groups are shown in Table 2. Equation (24) does not appear to be as good an overall description of the experimental measurements as Eqn (5), even when limited to energies above 150 eV.

CONCLUSIONS

The IMFPs of electrons in solids obey a universal curve which, for elements with energies, E, between 1 and 10 000 eV above the Fermi level, is described by

$$\lambda_m = \frac{538}{E^2} + 0.41(aE)^{1/2} \text{ monolayers}$$

where a is the monolayer thickness in nanometres. The RMS scatter factor is 1.59 overall but reduces to 1.36 for energies above 150 eV. For inorganic compounds

$$\lambda_m = \frac{2170}{E^2} + 0.72(aE)^{1/2} \text{ monolayers}$$

with an RMS scatter factor of 1.40 overall reducing to 1.38 for energies above 150 eV. For organic compounds the data are more scarce and the least scatter occurs for

$$\lambda_d = \frac{49}{E^2} + 0.11E^{1/2} \text{ mg m}^{-2}$$

with an RMS scatter factor of 2.1. For gases it is best to use the nearest equivalent of the above equations.

The above three equations currently represent the most accurate procedure for determining IMFPs and as such are recommended for use in the general quantification of surface spectroscopy.

The general predictions of Penn, for elements, show a slightly greater mean error and a 20% greater RMS scatter than the above empirical relation. The higher scatter appears to be associated with a stronger energy dependence than that exhibited by the experimental results. For inorganic compounds Penn's predictions are a factor of 1.9 too low with a 46% greater RMS scatter than the empirical relation, again with too strong an energy dependence. The calculations of Leckey *et al.*, whilst being of similar accuracy to the empirical relations, again show the stronger energy dependence. More measurements are therefore required at the highest possible energy to distinguish between these two possible energy dependences. Measurements are also required for alkali metals to test for any N_v dependence and measurements for compounds by several different laboratories would enable the general differences in IMFP magnitude between elements and inorganic compounds to be clarified.

Acknowledgements

The authors would like to thank those who provided data for the compilation and who, on many occasions, provided material prior to publication as well as stimulating discussions. Their names are too numerous to list but include many of those appearing in the Appendix.

REFERENCES

1. C. D. Wagner, *Anal. Chem.* **44**, 1050 (1972).
2. C. K Jørgensen and H. Berthou, *Discuss. Faraday Soc.* **54**, 269 (1972).
3. V. I. Nefedov, N. P. Sergushin, I. M. Band and M. B. Trzhaskovskaya, *J. Electron Spectrosc.* **2**, 383 (1973).
4. H. Berthou and C. K. Jørgensen, *Anal. Chem.* **47**, 482 (1975).
5. M. Janghorbani, M. Vulli and K. Starke, *Anal. Chem.* **47**, 2200 (1975).
6. V. I. Nefedov, N. P. Sergushin, Y. V. Salyn, I. M. Band and M. B. Trzhaskovskaya, *J. Electron Spectrosc.* **7**, 175 (1975).
7. C. C. Chang, *Surf. Sci.* **48**, 9 (1975).
8. P. M. Hall, J. M. Morabito and D. K. Conley, *Surf. Sci.* **62**, 1 (1977).
9. L. E. Davis, N. C. Macdonald, P. W. Palmberg, G. E. Riach and R. E. Weber, *Handbook of Auger Electron Spectroscopy*, 2nd Edn. Physical Electronics Industries Inc., Minnesota (1976).
10. M. P. Seah, *Surf. Sci.* **32**, 703 (1972).
11. J. C. Shelton, *J. Electron Spectrosc.* **3**, 417 (1974).
12. I. Lindau and W. E. Spicer, *J. Electron Spectrosc.* **3**, 409 (1974).
13. C. J. Powell, *Surf. Sci.* **44**, 29 (1974).
14. G. W. C. Kaye and T. H. Laby, *Tables of Physical and Chemical Constants*, 14th Edn. Longman, London (1973).
15. R. C. Weast (ed.), *Handboook of Chemistry and Physics*, 58th Edn. CRC Press, Cleveland, Ohio (1977–78).
16. D. M. Smith and T. E. Gallon, *J. Phys. D* **7**, 151 (1974).

17. D. Norman and D. P. Woodruff, Daresbury report DL/SRF/P100, *Surf. Sci.* submitted for publication.
18. M. P. Seah, *Surf. Sci.* **17**, 132 (1969).
19. W. J. Krolikowski and W. E. Spicer, *Phys. Rev. B* **1**, 478 (1970).
20. O. Hachenberg and W. Brauer, *Adv. Electron. Electron Phys.* **11**, 413 (1959).
21. J. J. Quinn, *Phys. Rev.* **126**, 1453 (1962).
22. S. M. Sze, J. L. Moll and T. Sugano, *Solid-State Electron.* **7**, 509 (1964).
23. D. R. Penn, *Phys. Rev. B* **13**, 5248 (1976).
24. D. R. Penn, *J. Electron Spectrosc.* **9**, 29 (1976).
25. F. L. Battye, J. G. Jenkin, J. Liesegang and R. C. G. Leckey, *Phys. Rev. B* **9**, 2887 (1974).
26. J. Szajman, J. Liesegang, R. C. G. Leckey and J. G. Jenkin, *Phys. Rev. B* to be published.

Accepted 30 October 1978

APPENDIX

References used in the compilation, in chronological order, with lists of materials studied in each reference.

*1. G. W. Gobeli and F. G. Allen, *Phys. Rev.* **127**, 141 (1962) (Si).
*2. S. M. Sze, J. L. Moll and T. Sugano, *Solid-State Electron.* **7**, 509 (1964). (Au).
*3. K. Siegbahn, C. Nordling, A. Fahlman, R. Nordberg, K. Hamrin, J. Hedman, G. Johansson, T. Bergmark, S.-E. Karlsson, I. Lindgren and B. Lindberg, *ESCA–Atomic, Molecular and Solid State Structure Studied by Means of Electron Spectroscopy*. Almqvist and Wiksells, Uppsala (1967). ($C_{18}H_{35}IO_2$ (α-iodostearic acid)).
*4. P. W. Palmberg and T. N. Rhodin, *J. Appl. Phys.* **39**, 2425 (1968). (Ag).
*5. J. L. Shay and W. E. Spicer *Phys. Rev.* **169**, 650 (1968). (CdS, CdSe, CdTe).
*6. B. L. Henke, *Adv. X-Ray Anal.* **13**, 1 (1970). ($C_{18}H_{36}O_2$ (stearic acid)).
*7. H. Kanter, *Phys. Rev. B* **1**, 522 (1970). (Ag, Al, Au).
*8. W. F. Krolikowski and W. E. Spicer, *Phys. Rev. B* **1**, 478 (1970). (Au).
*9. H. Kanter, *Phys. Rev. B* **1**, 2357 (1970). (Al).
*10. D. E. Eastman, *Solid State Commun.* **8**, 41 (1970). (Y).
*11. Y. Baer, P. F. Heden, J. Hedman, M. Klasson and C. Nordling, *Solid State Commun.* **8**, 1479 (1970). (Au).
*12. J. W. T. Ridgway and D. Haneman, *Surf. Sci.* **24**, 451 (1971). (Fe).
*13. K. Jacobi and J. Holzl, *Surf. Sci.* **26**, 54 (1971). (C).
*14. J. W. T. Ridgway and D. Haneman, *Surf. Sci.* **26**, 683 (1971). (Ni).
*15. M. P. Seah, *Surf. Sci.* **32**, 703 (1972). (Ag, Be, Cu).
*16. B. L. Henke, *Phys. Rev. A* **6**, 94 (1972). (Au).
*17. R. G. Steinhardt, J. Hudis and M. L. Perlman, *Phys. Rev. B* **5**, 1016 (1972). (C).
*18. P. Nielsen, *Phys. Rev. B* **6**, 3739 (1972). (Se).
*19. M. Klasson, J. Hedman, A. Berndtsson, R. Nilsson, C. Nordling and P. Melnik, *Phys. Scr.* **5**, 93 (1972). (Al_2O_3, Au).
*20. T. A. Carlson and G. E. McGuire, *J. Electron Spectros.* **1**, 161 (1972). (WO_3, W).
*21. H. Ebel and M. F. Ebel, *X-Ray Spectrom.* **2**, 19 (1973). (Au).
*22. J. P. Biberian and G. E. Rhead, *J. Phys. F* **3**, 675 (1973). (Pb).
*23. M. P. Seah, *J. Phys. F* **3**, 1538 (1973). (Cu).
*24. D. C. Jackson, T. E. Gallon and A. Chambers, *Surf. Sci.* **36**, 381 (1973). (Ag).
*25. W. A. Fraser, J. V. Florio, W. N. Delgass and W. D. Robertson, *Surf. Sci.* **36**, 661 (1973). (Cs).
*26. M. P. Seah, *Surf. Sci.* **40**, 595 (1973). (Sn).
*27. W. Pong and J. A. Smith, *J. Appl. Phys.* **44**, 174 (1973). (copper phthalocyanine).
*28. M. L. Tarng and G. K. Wehner, *J. Appl. Phys.* **44**, 1534 (1973). (Mo, W).
*29. C. J. Todd and R. Heckingbottom, *Phys. Lett. A* **42**, 455 (1973). (GeO_2).
*30. S. Thomas and T. W. Haas, *J. Vac. Sci. Technol.* **10**, 218 (1973). (Cs, K, Na, Rb).
*31. C. R. Brundle, *J. Vac. Sci. Technol.* **11**, 212 (1974). (CO, O_2).
*32. P. B. Needham and T. J. Driscoll, *J. Vac. Sci. Technol.* **11**, 278 (1974). (Fe_3O_4).
*33. J. C. Tracy, *J. Vac. Sci. Technol.* **11**, 280 (1974). (Al).
*34. F. L. Battye, J. G. Jenkin, J. Liesegang and R. C. G. Leckey, *Phys. Rev. B* **9**, 2887 (1974). (Al_2O_3).
*35. M. Klasson, A. Berndtsson, J. Hedman, R. Nilsson, R. Nyholm and C. Nordling, *J. Electron Spectrosc.* **3**, 427 (1974). (SiO_2, Si).
*36. J. Brunner and H. Zogg, *J. Electron. Spectrosc.* **5**, 911 (1974). (Au).
*37. F. L. Battye, J. Liesegang, R. C. G. Leckey and J. G. Jenkin, *J. Phys. C* **7**, L390 (1974). (NaCl).
*38. P. H. Holloway and J. B. Hudson, *Surf. Sci.* **43**, 123 (1974). (NiO).
*39. J. Perdereau, J. P. Biberian and G. E. Rhead, *J. Phys. F* **4**, 798 (1974). (Pb).
*40. J. T. Yates and N. E. Erickson, *Surf. Sci.* **44**, 489 (1974). (Xe).
*41. R. Flitsch and S. I. Raider, *J. Vac. Sci. Technol.* **12**, 305 (1975). (SiO_2, Si).
*42. P. H. Holloway, *J. Vac. Sci. Technol.* **12**, 1418 (1975). (Cr_2O_3).
*43. R. A. Armstrong, *Surf. Sci.* **50**, 615 (1975). (Ti).
*44. P. Nielsen, D. J. Sandman and A. J. Epstein, *Solid State Commun.* **17**, 1067 (1975). (tetracyanoquinodimethane, tetrathiofulvalene).
*45. F. L. Battye, J. Liesegang, R. C. G. Leckey and J. G. Jenkin, *Phys. Rev. B* **13**, 2646 (1976). (NaF).
*46. I. Lindau, P. Pianetta, K. Y. Yu and W. E. Spicer, *J. Electron Spectrosc.* **8**, 487 (1976). (Au).
*47. J. M. Hill, D. G. Royce, C. S. Fadley, L. F. Wagner and F. J. Grunthauer, *Chem. Phys. Lett.* **44**, 225 (1976). (SiO_2, Si).
*48. A. Yu. Mityagin, V. V. Panteleyev and N. Ya. Cherevatskiy, *Radio Eng. Electron. Phys.* **21**(3), 112 (1976). (In).
*49. S. Evans, R. G. Pritchard and J. M. Thomas, *J. Phys. C* **10**, 2483 (1977). (Ag, Au, C(diamond), C(graphite), $C_{18}H_{36}O_2$(stearic acid), Co, Cr, Cu, Fe, Ni, Si, V, Zn, graphite fluoride (Cf), polyethylene (low or high density), polyethylene terephthalate, polystyrene, polytetrafluoroethylene, polyvinyl chloride).
*50. R. L. Benbow and Z. Huryeh, *Phys. Lett. A* **60**, 253 (1977). (Bi).
*51. D. Norman and D. P. Woodruff, *Solid State Commun.* **22**, 711 (1977). (Au).
*52. D. T. Clark and H. R. Thomas, *J. Polym. Sci.*, to be published. (polybromoparaxylylene, polychloroparaxylylene, polyparaxylylene).
*53. D. T. Clark and D. Shuttleworth, *J. Polym. Sci.*, to be published. (polyvinylidene fluoride).
*54. C. J. Powell, R. J. Stein, P. B. Needham and T. J. Driscoll, *Phys. Rev. B* **16**, 1370 (1977). (Al, Be).
*55. T. Hattori, *Thin Solid Films* **46**, 47 (1977). (Pt).
*56. R. Bailey and J. E. Castle, *J. Mater. Sci.* **12**, 2049 (1977). (butylamine).
*57. A. Sepulveda and G. E. Rhead, *Surf. Sci.* **66**, 436 (1977). (Pb).
*58. J. Szajman, J. Liesegang, R. C. G. Leckey and J. G. Jenkin, *Phys. Rev. B* to be published (1978). (KI).
*59. J. Szajman, J. G. Jenkin, J. Liesegang and R. C. G. Leckey, *J. Electron Spectrosc.* **14**, 41 (1978). (Ge).